

Global model reduction for flows with moving boundary

Haotian Gao*, Mingjun Wei†

New Mexico State University, Las Cruces, NM 88003

Traditional POD-Galerkin projection, as a popular approach for model order reduction, is usually applied in a fixed fluid domain which, however, is not the case for many fluid-solid systems with moving objects/boundaries. Instead of treating a time-dependent fluid domain, we consider the combination of fluid and solid one single stationary domain. The idea, which is similar to immersed boundary technique used in numerical simulation, is to have a modified Navier-Stokes equation in a combined fluid-solid domain and add extra body-force terms to the equation with support only in solid area to represent the moving boundary or solid structure. Global POD modes can then be computed with a new inner product also defined in the combined domain. With both the modes and equations defined in a fixed fluid-solid domain, the Galerkin projection is applied directly in the same domain and provides a global reduced-order model for the system. In comparison to the traditional approach, the new global model ends up with extra terms to represent solid motion. The critical role of these new terms is demonstrated here in application to flows passing respectively an oscillatory two-dimensional cylinder and an oscillatory three-dimensional sphere, where the new terms clearly help to sustain overall system energy.

I. Introduction

With advances in computational science and engineering, high-fidelity numerical simulation has become a powerful tool in the study of natural flyers/runners/swimmers and man-made aerial/ground/underwater vehicles. However, its computational cost is still too high for many applications which require real-time control or numerous iterations for design and optimization in large parametric space. In those situations, reduced-order models (ROM) become handy to approximate the results with much less computational cost. Models at very low dimension also allow direct application of tools from dynamical system and control theory [1, 2].

Since its introduction to fluid mechanics community [3, 4], proper orthogonal decomposition (POD)-Galerkin projection has quickly become one of the most popular “top-down” approaches for model reduction of many fluid problems [5–15]. However, model reduction by POD-Galerkin projection faces a new challenge when there are moving solid boundaries or structures in fluid flow. With moving boundaries, when POD is applied to the flow field in a traditional manner, there is an inconsistency of coordinates for near-field dynamics (moving) and far-field dynamics (inertial). As it is reviewed recently [16], actuation modes [17, 18] and Eulerian-Lagrangian dynamic mesh adaptation methods [19–22] have been proposed to allow the transition between the moving/deforming near field to the stationary far field. There was also a different route taken by Liberge and Hamdouni, where they considered a fictitious stationary domain including both fluid and solid and applied POD-Galerkin projection on a modified equation for both fluid and solid [23]. Their approach shares some similarity as in our earlier effort [24] and more complete work presented in this paper, where we also considered both fluid and solid in a combined stationary domain. We borrow the idea from immersed boundary technique used in numerical simulation [25–27], where the effect of moving boundary is represented as extra bodyforce terms added to the original Navier-Stokes equation, and then develop a global POD-Galerkin projection in a fixed domain with moving bodyforce terms for boundaries.

*Research Assistant, Department of Mechanical and Aerospace Engineering

†Associate Professor, Department of Mechanical and Aerospace Engineering, Senior Member AIAA

Different from the approach of Liberge and Hamdouni [23], our method allows large and arbitrary movement of boundaries though only prescribed motion is considered at this moment.

For the rest of the paper, there are the proposed methodology in §II, the application to both two-dimensional and three-dimensional cases in §III, and the conclusion in §IV.

II. Basic methodology

In this section, for completeness, we will first review some basics of model reduction for traditional fluid flows: Galerkin projection and proper orthogonal decomposition (POD). Then, we will introduce our method of global model reduction for flows with moving boundaries.

II.A. Galerkin projection

The idea of Galerkin projection is to project the functions defining the original equation onto a finite-dimensional subspace of the full phase space [4]. To perform Galerkin projection, the phase space \mathcal{X} must be an inner product space spanned by a suitable set of basis functions. The suitable choices for basis functions include *mathematical modes*, such as Fourier modes and Chebyshev polynomials, as well as *empirical modes*, such as POD modes. For demonstration, consider simple dynamics described by

$$\dot{\mathbf{u}} = f(\mathbf{u}), \quad (1)$$

where f is a general operator linear or nonlinear on u . $u(x, t)$ can be expanded in terms of suitable orthogonal basis functions of \mathcal{X} (e.g. POD modes):

$$\mathbf{u}(x, t) = \sum_{k=1}^{\infty} a_k(t) \phi_k(x), \quad (2)$$

where the basis functions ϕ_k are often ordered by certain physical criteria: decreasing captured energy as for POD modes; increasing wavenumber (decreasing scale) as for Fourier modes; etc. Projecting the equation onto the set of basis functions, we get the dynamics of time coefficients:

$$\dot{a}_j = \langle f(\mathbf{u}), \phi_j \rangle, \quad j = 1, \dots, \infty. \quad (3)$$

The finite truncation in expansion and projection then gives a model equation of lower dimension. The truncation order will depend on the properties of original equations and the requirements of specific problems.

II.B. Proper orthogonal decomposition

Proper orthogonal decomposition (POD) was proved the most efficient way of capturing the dominant components of an infinite-dimensional process with finite and often only a few number of modes [4]. The goal for POD is to find an *optimal* subspace of finite dimension to present an ensemble of data $u(t) \in H$, where H is a Hilbert space with inner product $\langle \cdot, \cdot \rangle$. The *optimality* here can be defined by the minimization of the average error $\overline{\|u - u_s\|}$ between the original data $u(t)$ and the reconstruction from the subspace $u_s(t) = \sum_j \langle u, \phi_j \rangle \phi_j$, where $\overline{\cdot}$ denotes a time average and $\|\cdot\|$ is the induced norm on H . The basis functions ϕ_j are normally known as POD modes, and they are eigenvectors of the following eigenvalue problem:

$$\mathcal{R}\phi = \lambda\phi, \quad (4)$$

where $\mathcal{R} = \overline{u \otimes u}$. It is noticed that $u \otimes v$ is defined by

$$(u \otimes v)\psi = \langle \psi, v \rangle u \quad (5)$$

and depends on the definition of inner product. In most numerical simulations, the method of snapshots [28] is often used when the number of snapshots M and the number of spacial grid points N satisfies: $M \ll N$. The method of snapshots solves an M -dimensional eigenvalue problem instead of the original N -dimensional eigenvalue problem (4) and achieves the same first M modes.

II.C. Traditional POD-Galerkin projection for fluid flows

Using POD together with Galerkin projection, we have a systematic procedure to obtain ROMs from simulation or experimental data. For traditional fluid mechanics problems, the approach can be applied on Navier-Stokes equation [4, 5]:

$$\frac{\partial \mathbf{u}}{\partial t} + \mathbf{u} \cdot \nabla \mathbf{u} = -\nabla p + \frac{1}{\text{Re}} \nabla^2 \mathbf{u}, \quad (6)$$

where \mathbf{u} is velocity vector, p is pressure, and Re is the Reynolds number. The velocity can be expanded about its mean value \mathbf{u}_0 and on POD modes ϕ_j as

$$\mathbf{u} \approx \mathbf{u}^N = \mathbf{u}_0 + \sum_{j=1}^N a_j(t) \phi_j(\mathbf{x}), \quad (7)$$

where the finite truncation at $j = N$ is performed for low-dimensional modeling. Substitute (7) in (6) and project the equation one to bases ϕ_i to get dynamic equations for time coefficients,

$$\dot{a}_i = \frac{1}{\text{Re}} \sum_{j=0}^N l_{ij} a_j + \sum_{j=0}^N \sum_{k=0}^N q_{ijk} a_j a_k, \quad i = 1, \dots, N, \quad (8)$$

where $l_{ij} = \langle \nabla^2 \phi_j, \phi_i \rangle_{\Omega}$ and $q_{ijk} = \langle \nabla \cdot (\phi_j \phi_k), \phi_i \rangle_{\Omega}$. $\phi_0 = \mathbf{u}_0$ and $a_0 = 1$ are introduced here for simple notation. In (8), orthogonality has been applied and the pressure term has been cancelled by appropriate boundary conditions (e.g. periodic condition).

II.D. Global POD-Galerkin projection for flows with moving boundary

The traditional approach of POD-Galerkin projection requires fixed fluid domain, which is not the case for flows with moving solid boundaries and structures. Instead of considering a time-dependent fluid domain, we treat the combination of fluid and solid as one whole stationary domain. The idea is similar to immersed boundary technique used in numerical simulation [25–27], where the combined domain allows simple fixed meshes for discretization and the effect of moving boundary/structure is represented as extra body-force terms added to the original Navier-Stokes equation on specific “solid” area. Here, it is similar to immersed boundary method that the global Galerkin projection is based on a modified Navier-Stokes equation for the combined domain [29–31]:

$$\frac{\partial \mathbf{u}}{\partial t} + \mathbf{u} \cdot \nabla \mathbf{u} = -\nabla p + \frac{1}{\text{Re}} \nabla^2 \mathbf{u} + \mathbf{f}, \quad (9)$$

where \mathbf{f} is the extra bodyforce term added in solid domain Ω_s to define the trajectory of solid boundary/structure:

$$\mathbf{f} = \begin{cases} (\mathbf{u} \cdot \nabla \mathbf{u} - \frac{1}{\text{Re}} \nabla^2 \mathbf{u})^n + \frac{1}{\Delta t} (\mathbf{V} - \mathbf{u}^n) & \text{in } \Omega_s \\ 0 & \text{otherwise} \end{cases}, \quad (10)$$

with \mathbf{V} being the prescribed velocity of solid, the pressure term has been neglected.

With the modified fluid-solid equation (9), the classical approach for fixed fluid domain can be directly applied on the whole fluid-solid domain to get

$$\dot{a}_i = \sum_{j=0}^N \left(\frac{1}{\text{Re}} l_{ij} - l'_{ij} \right) a_j - \sum_{j=0}^N \sum_{k=0}^N (q_{ijk} - q'_{ijk}) a_j a_k + c_i, \quad i = 1, \dots, N, \quad (11)$$

which is similar to the traditional form in (8). However, the new dynamic equation (11) has some new parameters defined by inner products with support only in solid domain:

$$l'_{ij} = \left\langle \left(\frac{1}{\text{Re}} \nabla^2 \phi_j + \frac{1}{\Delta t} \phi_j \right), \phi_i \right\rangle_{\Omega_s(t)}, \quad (12)$$

$$q'_{ijk} = \langle \nabla \cdot (\phi_j \phi_k), \phi_i \rangle_{\Omega_s(t)}, \quad (13)$$

$$c_i = \left\langle \frac{1}{\Delta t} \mathbf{V}^n, \phi_i \right\rangle_{\Omega_s(t)}, \quad (14)$$

and old parameters with similar definition but being extended to with support in the entire combined domain with both fluid and solid. It is worth noting that the corresponding global POD modes are also defined by inner products in the combined fluid-solid domain without telling difference between fluid and solid. For simplicity, we keep the same weight for the energy contribution from fluid and solid area in the definition of inner product, however, it is possible to consider fluid and solid with different weight and the change may improve the global POD modes for better ROM performance. The resulted model (11) describes globally both fluid and solid. Different from the approach of Liberge and Hamdouni [23], our method allows large and arbitrary movement of boundaries though only prescribed motion is considered at this moment.

III. Application and results for 2D and 3D flows

In this section, our approach of global model reduction is applied first on a flow passing a 2D oscillatory cylinder then on a flow passing a 3D oscillatory sphere.

III.A. Flow passing a 2D oscillatory cylinder

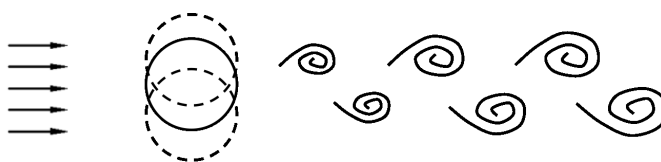


Figure 1. A schematic of flow passing an oscillatory cylinder.

As sketched in figure 1, a two-dimensional cylinder oscillates (along y) normal to the incoming flow. The Reynolds number is 100, which is defined by the incoming velocity and cylinder diameter. The computational domain is $l_x \times l_y = (0, 50) \times (0, 30)$ with uniform mesh at $N_x \times N_y = 1000 \times 600$, and the neutral position of the cylinder center is at $(x_0, y_0) = (10, 15)$. The oscillation is defined by $y(t) = y_0 + A \sin(2\pi ft)$ with amplitude $A = 1.5$ and frequency $f = 0.2$. Here, the large amplitude is picked intentionally to challenge the capability of our approach to handle large domain change. The numerical algorithm is the same as the one reported and tested in our previous numerical simulations [30, 31], where the projection method is applied to solve incompressible Navier-Stokes equations [32], the 3rd-order Runge-Kutta method is used for time advancement, and the immersed boundary method is implemented to describe moving boundaries/structures [27].

With the chosen amplitude and frequency, the wake vortex structure from our simulation shows P+S pattern (figure 2), which matches the prediction from classical parametric study by Williamson [33].

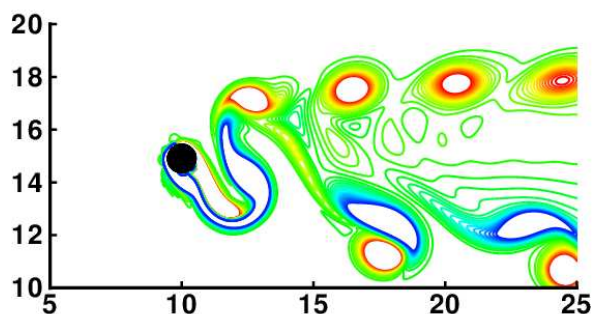


Figure 2. A snapshot at $T = 5$ from direct numerical simulation: vorticity is marked by contours.

Global POD modes were then computed from 400 snapshots of above simulation data which covers 4 time periods of oscillation. The results are shown in figure 3: the energy efficiency of POD is clearly indicated by the energy spectrum in figure 3 (a); both the energy distribution and the individual POD modes (figure 3 c-f) show the pairing between mode 1 & 2 and mode 3 & 4, which is typically seen in POD modes of convection-dominant flows.

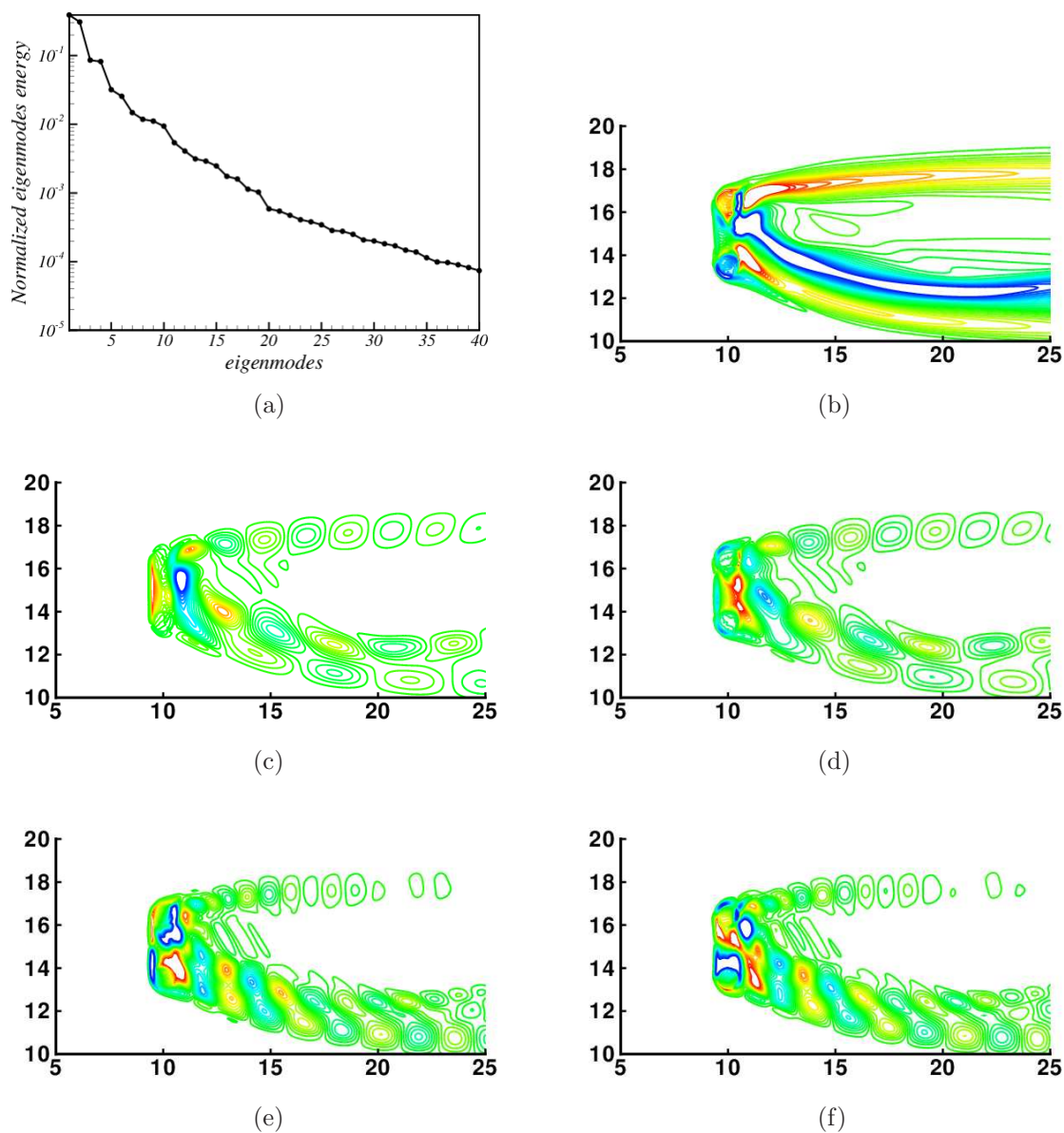


Figure 3. The energy distribution and most energetic modes (shown by vorticity contours) from POD analysis of flow passing an oscillatory cylinder: (a) the energy spectrum of POD modes; (b) mean flow; (c) mode 1; (d) mode 2; (e) mode 3; (f) mode 4.

The low-order dynamic system of the most energetic modes (i.e. currently first 8 modes) can then be achieved by the global projection onto these modes as we described earlier. In figure 4, we plot the phase portraits for coefficients (a_1, a_2) and (a_1, a_3) respectively, where, in each phase portrait, different lines and symbols indicates results from direct numerical simulation (considered as benchmark), our global model reduction (using forcing terms to represent solid motion), and the traditional POD-Galerkin projection (applied naively without forcing terms for solid motion). Our global approach shows the capability to capture basic dynamics and sustain the system energy by using the first 8 modes, while the one without forcing term can not sustain the system energy and the modes are quickly dissipated.

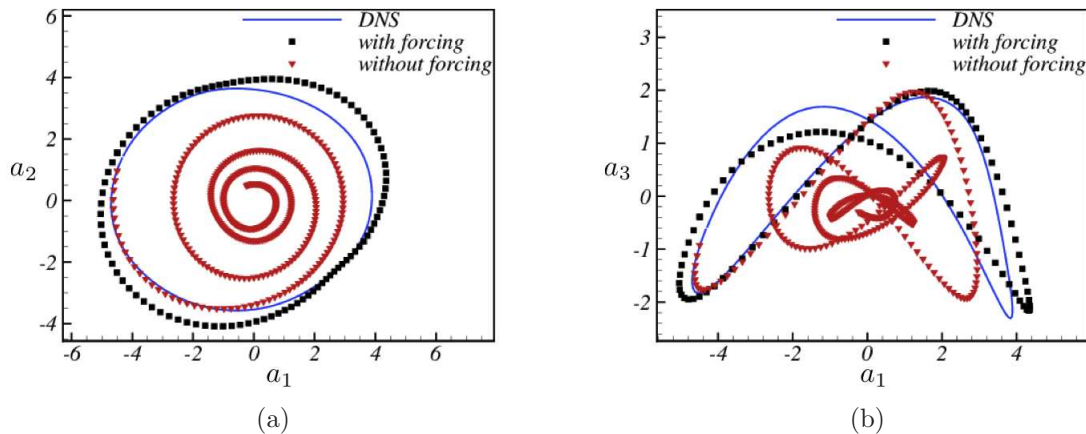


Figure 4. The phase portraits of: (a) (a_1, a_2) and (b) (a_1, a_3) , where the results computed from our current approach and the approach without forcing terms are benchmarked by the result from direct numerical simulation.

III.B. Flow passing a 3D oscillatory sphere

The same approach has been applied to a three-dimensional oscillatory sphere with incoming flow, which, together with the sphere diameter, defines the Reynolds number to be 300. The computational domain is $l_x \times l_y \times l_z = (-4, 8) \times (-4, 4) \times (-4, 4)$ with uniform mesh at $N_x \times N_y \times N_z = 300 \times 200 \times 200$, and the neutral position of the sphere center is at $(x_0, y_0, z_0) = (-1, 0, 0)$. The oscillation is along y and defined by $y(t) = y_0 + A \sin(2\pi ft)$ with amplitude $A = 1.0$ and frequency $f = 0.16$. We used the same numerical method and extended it to three-dimensional. Figure 5 shows a typical snapshot from our direct numerical simulation where vortex structures are shedding behind the sphere.

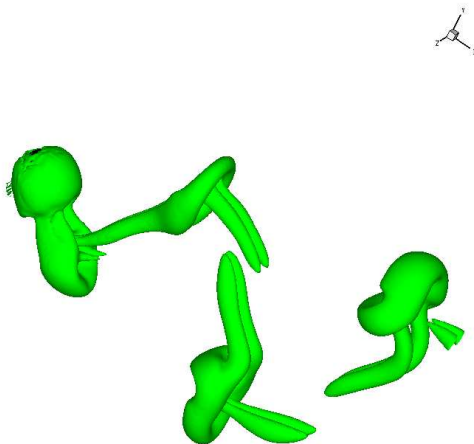


Figure 5. The vorticity structure of the flow passing a 3D oscillatory sphere.

Similarly, as shown in figure 6, the energy spectrum suggests the efficiency in energy capturing by global POD modes, and the same pairing pattern is observed from the energy level and shape of modes for the three-dimensional case.

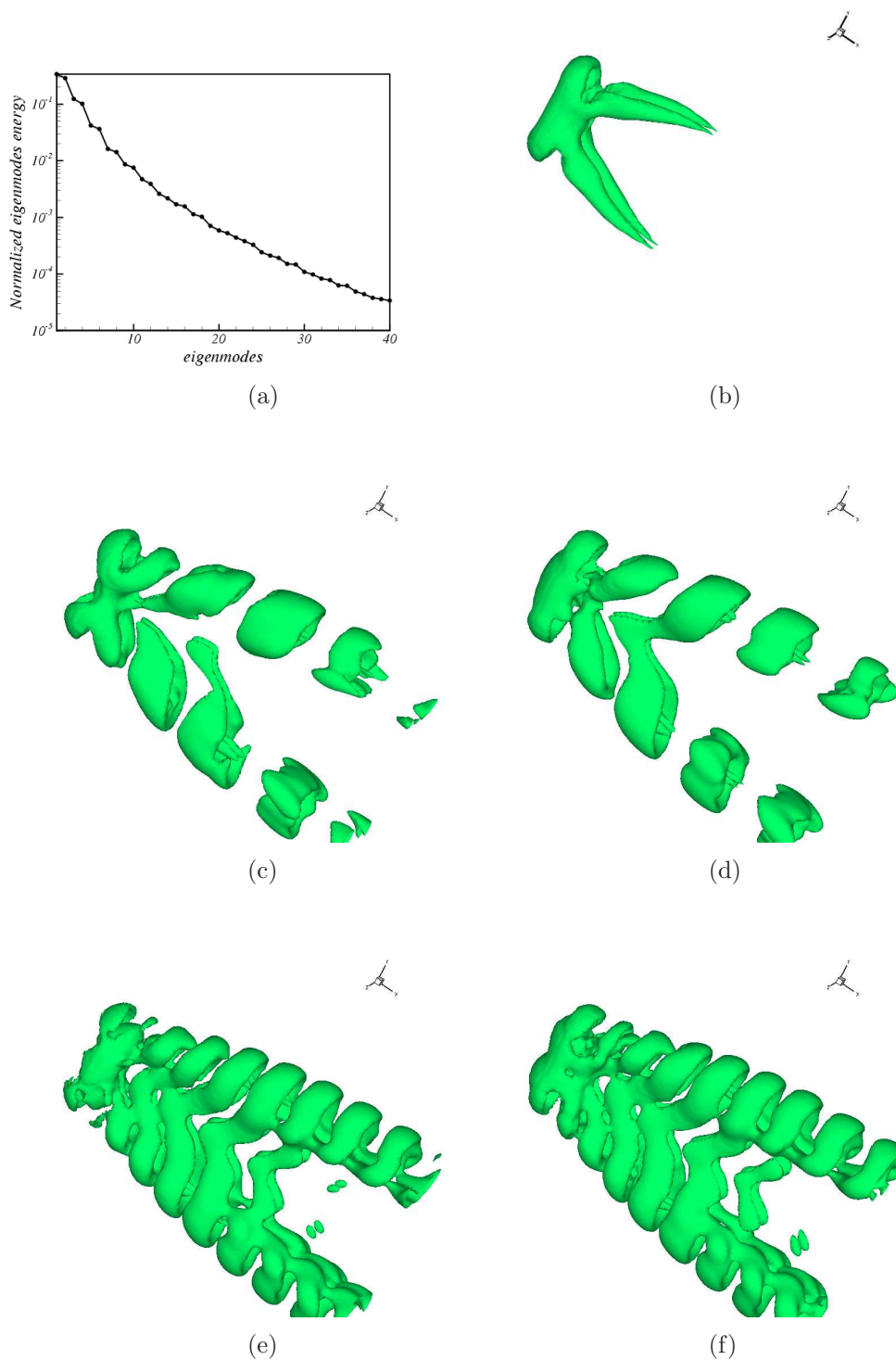


Figure 6. The energy distribution and most energetic modes (shown by iso-surface of Q criteria) from POD analysis of flow passing an oscillatory sphere: (a) the energy spectrum of POD modes; (b) mean flow; (c) mode 1; (d) mode 2; (e) mode 3; (f) mode 4.

Finally, figure 7 shows similar performance of the global fluid-solid model using the first 8 modes in the three-dimensional case. Our model behaves well by sustaining system energy through added forcing terms, which is derived directly from the modified Navier-Stokes equation with rigorously.

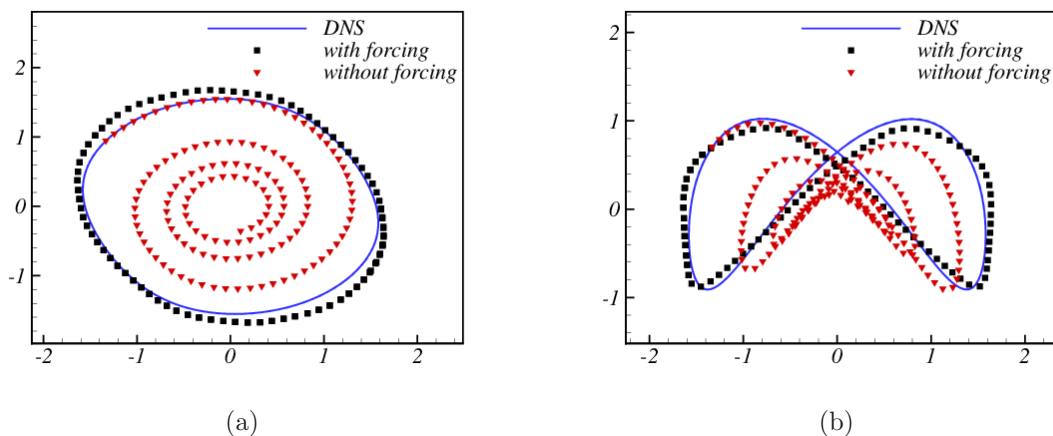


Figure 7. The phase portraits of: (a) (a_1, a_2) and (b) (a_1, a_3) , where the results computed from our current approach and the approach without forcing terms are benchmarked by the result from direct numerical simulation.

IV. Conclusion

We have developed a global approach for model order reduction of dynamic problems with both fluid flow and moving solid boundaries/bodies. The current approach is based on but different from traditional POD-Galerkin project method, which is usually applied on fluid flow with fixed domain. Using a similar idea of immersed boundary method for numerical simulation, we work on a modified Navier-Stokes equation for the combined fluid-solid domain with extra forcing terms for solid effects with support only in solid area. The POD modes are defined accordingly in the combined domain. With globally defined POD modes and Galerkin projection in the new fluid-solid domain, the rest of steps are straightforward by following the same way working for the fixed domain. The approach has been applied to both 2D and 3D cases with moving boundaries: flows passing respectively an oscillatory cylinder and an oscillatory sphere. For both cases, the global POD keeps its capability of capturing most energy of flow, and the resulted Galerkin modes can replicate basic dynamics by using first 8 modes. The added forcing term for solid boundary effects shows critical role in sustaining the overall system energy.

Acknowledgment

The authors gratefully acknowledge the support from Army Research Laboratory through Micro Autonomous System and Technology (MAST) CTA and Army High Performance Computing Research Center (AHPARC). HG would also thank the support by Graduate Research Enhancement Grant (GREG) of NMSU.

References

- ¹Dowell, E. H. and Hall, K. C., "Modeling of fluid-structure interaction," *Annual Review of Fluid Mechanics*, Vol. 33, No. 1, 2001, pp. 445–490.
- ²Rowley, C. W. and Williams, D. R., "Dynamics and control of high-Reynolds-number Flow over open cavities," *Ann. Rev. Fluid Mech.*, Vol. 38, 2006, pp. 251–276.
- ³Berkooz, G., Holmes, P., and Lumley, J. L., "The proper orthogonal decomposition in the analysis of turbulent flows," *Ann. Rev. Fluid Mech.*, Vol. 25, 1993, pp. 539–575.
- ⁴Holmes, P., Lumley, J. L., and Berkooz, G., *Turbulence, Coherent Structures, Dynamical Systems and Symmetry*, Cambridge University Press, Cambridge, 1996.
- ⁵Noack, B. R., Afanasiev, K., Morzynski, M., Tadmor, G., and Thiele, F., "A hierarchy of low-dimensional models for the transient and post-transient cylinder wake," *Journal of Fluid Mechanics*, Vol. 497, No. 1, 2003, pp. 335–363.
- ⁶Ma, X. and Karniadakis, G. E., "A low-dimensional model for simulating three-dimensional cylinder flow," *Journal of Fluid Mechanics*, Vol. 458, No. 1, 2002, pp. 181–190.
- ⁷Buffoni, M., Camarri, S., Iollo, A., Salvetti, M. V., et al., "Low-dimensional modelling of a confined three-dimensional wake flow," *Journal of Fluid Mechanics*, Vol. 569, 2006, pp. 141–150.

⁸Lieu, T. and Farhat, C., "Adaptation of aeroelastic reduced-order models and application to an F-16 configuration," *AIAA J.*, Vol. 45, No. 6, 2007, pp. 1244–1257.

⁹Siegel, S. G., Seidel, J., Fagley, C., Luchtenburg, D., Cohen, K., and McLaughlin, T., "Low-dimensional modelling of a transient cylinder wake using double proper orthogonal decomposition," *Journal of Fluid Mechanics*, Vol. 610, No. 1, 2008, pp. 1–42.

¹⁰Wei, M. and Rowley, C. W., "Low-dimensional models of a temporally evolving free shear layer," *J. Fluid Mech.*, Vol. 618, 2009, pp. 113–134.

¹¹Rowley, C. W. and Marsden, J. E., "Reconstruction Equations and the Karhunen-Loève Expansion for Systems with Symmetry," *Phys. D*, Vol. 142, 2000, pp. 1–19.

¹²Rowley, C. W., Colonius, T., and Murray, R. M., "Model reduction for compressible flow using POD and Galerkin projection," *Phys. D*, Vol. 189, No. 1–2, Feb. 2004, pp. 115–129.

¹³Noack, B. R., Schlegel, M., Morzyński, M., and Tadmor, G., "System reduction strategy for Galerkin models of fluid flows," *International Journal for Numerical Methods in Fluids*, Vol. 63, No. 2, 2010, pp. 231–248.

¹⁴Wei, M., Qawasmeh, B. R., Barone, M., van Bloemen Waanders, B. G., and Zhou, L., "Low-dimensional model of spatial shear layers," *Physics of Fluids*, Vol. 24, No. 1, 2012, pp. 014108.

¹⁵Cammilleri, A., Guéniat, F., Carlier, J., Pastur, L., Memin, E., Lusseyran, F., and Artana, G., "POD-spectral decomposition for fluid flow analysis and model reduction," *Theoretical and Computational Fluid Dynamics*, 2013, pp. 1–29.

¹⁶Tadmor, G., Lehmann, O., Noack, B. R., and Morzyński, M., "Galerkin models enhancements for flow control," *Reduced-Order Modelling for Flow Control*, Springer, 2011, pp. 151–252.

¹⁷Noack, B. R., Tadmor, G., and Morzynski, M., "Actuation models and dissipative control in empirical Galerkin models of fluid flows," *American Control Conference, 2004. Proceedings of the 2004*, Vol. 6, IEEE, 2004, pp. 5722–5727.

¹⁸Tadmor, G. and Noack, B. R., "Dynamic estimation for reduced Galerkin models of fluid flows," *American Control Conference, 2004. Proceedings of the 2004*, Vol. 1, IEEE, 2004, pp. 746–751.

¹⁹Anttonen, J., King, P., and Beran, P., "POD-based reduced-order models with deforming grids," *Mathematical and computer modelling*, Vol. 38, No. 1, 2003, pp. 41–62.

²⁰Anttonen, J., King, P., and Beran, P., "Applications of multi-POD to a pitching and plunging airfoil," *Mathematical and computer modelling*, Vol. 42, No. 3, 2005, pp. 245–259.

²¹Feng, Z. and Soulaïmani, A., "Nonlinear aeroelasticity modeling using a reduced order model based on proper orthogonal decomposition," *ASME Pressure Vessels and Piping Division Conference*, No. 26006, 2007.

²²Liberge, E., Benaouicha, M., and Hamdouni, A., "Proper orthogonal decomposition investigation in fluid structure interaction," *European Journal of Computational Mechanics/Revue Européenne de Mécanique Numérique*, Vol. 16, No. 3-4, 2007, pp. 401–418.

²³Liberge, E. and Hamdouni, A., "Reduced order modelling method via proper orthogonal decomposition (POD) for flow around an oscillating cylinder," *Journal of Fluids and Structures*, Vol. 26, No. 2, 2010, pp. 292–311.

²⁴Wei, M. and Yang, T., "A global approach for reduced-order models of flapping flexible wings," AIAA paper 2010-5085, Chicago, IL, 2010.

²⁵Peskin, C. S., "Flow patterns around heart valves: a numerical method," *J. Comput. Phys.*, Vol. 10, No. 2, 1972, pp. 252–271.

²⁶Peskin, C. S., "Numerical analysis of blood flow in the heart," *J. Comput. Phys.*, Vol. 25, No. 3, 1977, pp. 220–252.

²⁷Mohd-Yusof, J., "Combined immersed-boundary/B-spline methods for simulations of flow in complex geometries," Center for Turbulence Research, Annual Research Briefs – 1997, 1997.

²⁸Sirovich, L., "Chaotic dynamics of coherent structures. Parts I–III," *Quarterly of Applied Math.*, Vol. XLV, No. 3, 1987, pp. 561–582.

²⁹Zhao, H., Freund, J. B., and Moser, R. D., "A fixed-mesh method for incompressible flow-structure systems with finite solid deformations," *J. Comput. Phys.*, Vol. 227, 2008, pp. 3114–3140.

³⁰Yang, T., Wei, M., and Zhao, H., "Numerical study of flexible flapping wing propulsion," 48th AIAA Aerospace Sciences Meeting and Exhibit, Orlando, FL, AIAA paper 2010-0553, 2010.

³¹Xu, M., Wei, M., Yang, T., Lee, Y. S., and Burton, T. D., "Nonlinear Structural Response in Flexible Flapping Wings with Different Density Ratio," 49th AIAA Aerospace Sciences Meeting and Exhibit, Orlando, FL, AIAA paper 2011-376, 2011.

³²Brown, D. L., Cortez, R., and Minion, M. L., "Accurate projection methods for the incompressible Navier-Stokes equations," *J. Comput. Phys.*, Vol. 168, 2001, pp. 464–499.

³³Williamson, C., "Vortex dynamics in the cylinder wake," *Annual review of fluid mechanics*, Vol. 28, No. 1, 1996, pp. 477–539.